RSC Advances

ROYAL SOCIETY OF CHEMISTRY

www.rsc.org/advances

Sequential detection of mercury (II) and thiol-containing amino acids by a fluorescent chemosensor

Ga Rim You, Sun Young Lee, Jae Jun Lee, Yong Sung Kim, Cheal Kim*

Department of Fine Chemistry and Department of Interdisciplinary Bio IT Materials, Seoul National University of Science and Technology, Seoul 139-743, Korea. Fax: +82-2-973-9149; Tel: +82-2-970-6693; E-mail: chealkim@seoultech.ac.kr

Abstract

A simple fluorescent chemosensor **1** for the sequential detection of Hg^{2+} and cysteine or glutathione was developed by combination of thiosemicarbazide and 8-hydroxyjulolidine-9-carboxaldehyde. The sensor **1** exhibited an 'ON-OFF' fluorescent quenching response in the presence of Hg^{2+}, which was explained by theoretical calculations. **1** also showed high selectivity in the presence of potential competitors such as Ag^{+} and Pb^{2+}. Moreover, the resulting Hg^{2+}-2·**1** complex acted as an efficient 'OFF-ON' sensor for cysteine or glutathione, showing recovery of 2·**1** from Hg^{2+}-2·**1** complex. Therefore, the sensor **1** can be employed as a practical fluorescent chemosensor for recognition of Hg^{2+} and thiol-containing amino acids in aqueous solution.

Keywords: fluorescent chemosensor, sequential detection, mercury, cysteine, glutathione

1. Introduction

In recent years, considerable efforts have been devoted to the development of chemosensors for the selective detection of heavy metal ions with environmental and biological importance.[1-5] In particular, much attention has been paid to the detection of Hg^{2+} because it could cause a variety of symptoms in vivo.[6-7] Mercury is found in many products common to daily life, such as batteries, paints, and electronic equipment, and it exists in a variety of different forms (ionic, metallic, and as part of inorganic and organic salts and complexes). Whether in the inorganic mercury or its compounds, once consumed by humans,[8, 9] it can accumulate in the human body and a very small amount of mercury ions could cause serious diseases, such as cardiovascular disease, serious cognitive and motion disorders, Minamata disease and coronary heart disease.[10-15]

Cysteine (Cys) and glutathione (GSH) as intracellular thiol-containing amino acids play critical roles in biological systems.[16-20] Cys has been proven to act as a potential neurotoxin, a biomarker for various medical conditions, and a disease-associated physiological regulator.[21-23] A deficiency of Cys is related to many medical conditions including slow growth, hair depigmentation, edema, liver damage, muscle and fat loss, hematopoiesis decrease, leucocyte loss, psoriasis and skin lesions.[24] Also, abnormal levels of GSH can lead to cancer, aging, heart problems, and other ailments.[25, 26] Thus, the developments of sensory probes for a rapid, sensitive and selective analysis of the thiol-containing amino acids is highly demanded. Among them, the metal complex-based fluorescent chemosensors to selectively detect amino acids have attracted much attention.[18, 20, 27-34]

Quite recently, there has been a great emergence of interests in the development of chemosensors for the sequential detection of various cations and amino acids. [35-41] Among the sequential types of chemosensors, the probes based on fluorescent determination of Hg^{2+} and the thiol-containing amino acids have been sometimes used due to the thiophilic nature of Hg^{2+}. [30-36] Therefore, our group has been interested in the fluorescent sequential recognition of Hg^{2+} and the thiol-containing amino acids.

Herein, we describe a new compound **1** based on a julolidine moiety, which was

designed and synthesized as a fluorescent chemosensor of Hg^{2+}. The sensor **1** could detect Hg^{2+} by fluorescence quenching response with high selectivity in aqueous media. Subsequently, chemosensing ensemble Hg^{2+}-2·**1** showed highly selective detection to Cys or GSH via fluorescence enhancement by utilizing the mercury-thiol affinity.

2. Experimental

2.1. Materials and equipment

All the solvents and reagents (analytical and spectroscopic grade) were purchased from Sigma-Aldrich. ^{1}H and ^{13}C NMR spectra were recorded on a Varian 400 MHz and 100 MHz spectrometer and chemical shifts were recorded in ppm. Electro spray ionization mass spectra (ESI-MS) were collected on a Thermo Finnigan (San Jose, CA, USA) LCQ_{TM} Advantage MAX quadrupole ion trap instrument by infusing samples directly into the source using a manual method. Spray voltage was set at 4.2 kV, and the capillary temperature was at 80 ^{o}C. Absorption spectra were recorded at room temperature using a Perkin Elmer model Lambda L25 UV/Vis spectrometer. The emission spectra were recorded on a Perkin-Elmer LS45 fluorescence spectrometer. Elemental analysis for carbon, nitrogen, and hydrogen was carried out using a Flash EA 1112 elemental analyzer (thermo) at the Organic Chemistry Research Center of Sogang University, Korea.

*2.2. Synthesis of receptor **1***

An ethanolic solution of thiosemicarbazide (0.09 g, 1 mmol) was added to 8-hydroxyjulolidine-9-carboxaldehyde (0.19 g, 1.1 mmol) in absolute ethanol (3 mL). Two drops of HCl were added into the reaction solution and it was stirred for 12 h at room temperature. A yellow precipitate was filtered, washed several times with ethanol and diethyl ether, and dried in vacuum to obtain the pure yellow solid. Yield 0.20 g (69%); ^{1}H NMR (400 MHz DMSO-d_6, ppm): δ 10.99 (s, 1H), 9.37 (s, 1H), 8.05 (s, 1H), 7.74 (d, 2H), 6.70 (s, 1H), 3.15 (m, 4H), 2.59 (m, 4H), 1.84 (m, 4H); ^{13}C NMR (100 MHz, DMSO-d_6, 25 °C): δ = 178.79, 155.91, 150.11, 148.05, 131.15, 115.81, 109.24, 108.79, 52.15, 51.60, 29.33, 24.33, 23.87, 23.55, 23.30. ESI-MS m/z ($M+H^{+}$): calcd, 291.13; found, 291.07. Anal. Calc. for

$C_{14}H_{18}N_4OS$: C, 57.91; H, 6.25; N, 19.29%; Found: C, 57.97; H, 6.38; N, 19.33%.

2.3. Fluorescence and UV-vis titrations

For Hg^{2+}, **1** (2.9 mg, 0.01 mmol) was dissolved in dimethylsulfoxide (DMSO, 1 mL) and 3 μL of this solution (10 mM) was diluted with 2.997 mL of DMSO/bis-tris buffer (8/2, v/v; 10 mM bis-tris, pH = 7.0) to make the final concentration of 10 μM. $Hg(NO_3)_2 \cdot H_2O$ (3.4 mg, 0.01 mmol) was dissolved in DMSO (1 mL) and 0.3-7.8 μL of this Hg^{2+} solution (10 mM) was transferred to the receptor **1** solution (10 μM) prepared above. After mixing them for a few seconds, fluorescence and UV-vis spectra were taken at room temperature.

For Cys or GSH, **1** (2.9 mg, 0.01 mmol) was dissolved in DMSO (1 mL) and 3 μL of this solution (10 mM) was diluted with 2.994 mL of DMSO/bis-tris buffer (8/2, v/v) to make the final concentration of 10 μM. $Hg(NO_3)_2 \cdot H_2O$ (3.4 mg, 0.01 mmol) was dissolved in DMSO (1 mL) and 3 μL of this Hg^{2+} solution (10 mM) was transferred to each receptor solution (10 μM) to give 1 equiv. Then, Cys (2.4 mg, 0.02 mmol) or GSH (6.2 mg, 0.02 mmol) was dissolved in bis-tris buffer (10 mM, 1 mL) and 0.3-3.9 μL of the Cys or GSH solution (20 mM) was transferred to each complex solution (10 μM). After mixing them for a few seconds, fluorescence and UV-vis spectra were taken at room temperature.

2.4. Job plot measurements

For Hg^{2+}, **1** (2.9 mg, 0.01 mmol) was dissolved in DMSO (1 mL). 3, 2.7, 2.4, 2.1, 1.8, 1.5, 1.2, 0.9, 0.6, 0.3 and 0 μL of the **1** solution were taken and transferred to vials. Each vial was diluted with bis-tris buffer to make a total volume of 2.997 mL. $Hg(NO_3)_2 \cdot H_2O$ (3.4 mg, 0.01 mmol) was dissolved in DMSO (1 mL). 0, 0.3, 0.6, 0.9, 1.2, 1.5, 1.8, 2.1, 2.4, 2.7, and 3 μL of the $Hg(NO_3)_2$ solution were added to each diluted **1** solution. Each vial had a total volume of 3 mL. After reacting them for a few seconds, UV-vis spectra were taken at room temperature.

For Cys or GSH, **1** (2.9 mg, 0.01 mmol) was dissolved in DMSO (1 mL) and $Hg(NO_3)_2 \cdot H_2O$ (3.4 mg, 0.01 mmol) was dissolved in DMSO (1 mL), respectively. The two solutions were mixed to make Hg^{2+}-2·**1** complex. 3, 2.7, 2.4, 2.1, 1.8, 1.5, 1.2, 0.9, 0.6, 0.3 and 0 μL of the Hg^{2+}-2·**1** solution were taken and transferred to vials. Each vial was diluted

with bis-tris buffer to make a total volume of 2.997 mL. Cys (1.2 mg, 0.01 mmol) or GSH (3.1 mg, 0.01 mmol) was dissolved in bis-tris buffer (10 mM, 1 mL). 0, 0.3, 0.6, 0.9, 1.2, 1.5, 1.8, 2.1, 2.4, 2.7, and 3 μL of the Cys or GSH solution were added to each diluted Hg^{2+}-2·**1** solution. Each vial had a total volume of 3 mL. After reacting them for a few seconds, UV-vis spectra were taken at room temperature.

2.5. Competition experiments

For Hg^{2+}, **1** (2.9 mg, 0.01 mmol) was dissolved in DMSO (1 mL) and 3 μL of this solution (10 mM) was diluted with 2.994 mL of 10 mM bis-tris buffer to make the final concentration of 10 μM. MNO_3 (M = Na, K, Ag, 0.02 mmol) or $M(NO_3)_2$ (M = Mn, Co, Ni, Cu, Zn, Cd, Mg, Ca, Pb, 0.02 mmol) or $M(ClO_4)_2$ (M = Fe, 0.02 mmol) or $M(NO_3)_3$ (M = Fe, Cr, Al, Ga, In, 0.02 mmol) was separately dissolved in 10 mM bis-tris (1 mL). 1.5 μL of each metal solution (20 mM) was taken and added to 3 mL of the solution of receptor **1** (1 μM) to give 1 equiv of metal ions. Then, 1.5 μL of Hg^{2+} solution (20 mM) was added into the mixed solution of each metal ion and **1** to make 1 equiv. After mixing them for a few seconds, fluorescence spectra were taken at room temperature.

For Cys or GSH, **1** (2.9 mg, 0.01 mmol) was dissolved in DMSO (1 mL) and 3 μL of the **1** (10 mM) was diluted to 2.988 mL of 10 mM bis-tris buffer to make the final concentration of 1 μM. $Hg(NO_3)_2·H_2O$ (1.7 mg, 0.01 mmol) was dissolved in DMSO (1 mL). 3 μL of Hg^{2+} solution (10 mM) was taken and added into **1** solution (10 μM) to make mercury complex. Various amino acids and peptide such as Ala, Asn, Cys, Gln, Glu, Gly, His, Ile, Leu, Lys, Met, Phe, Pro, Ser, Trp, Val, Arg, Thr, Asp and GSH (0.02 mmol) were separately dissolved in 10 mM bis-tris buffer (20 mM). 3 μL of each amino acid and peptide solution (20 mM) was taken and added into each mercury complex solution prepared above to make 2 equiv. Then, 3 μL of the Cys or GSH solution (20 mM) was added into the mixed solution of each amino acid or peptide and mercury complex to make 2 equiv. After mixing them for a few seconds, fluorescence spectra were taken at room temperature.

2.6. ^1H NMR titrations

Four NMR tubes of receptor **1** (2.9 mg, 0.01 mmol) dissolved in DMSO-d_6 (700 μL)

were prepared and then four different concentrations (0, 0.005, 0.01, 0.02 mmol) of $Hg(NO_3)_2 \cdot H_2O$ dissolved in DMSO-d_6 were added to each solution of receptor **1**. After shaking them for a minute, ^{1}H NMR spectra were taken at room temperature.

*2.7. Theoretical calculation methods of **1** with Hg^{2+}*

All DFT/TDDFT calculations based on the hybrid exchange-correlation functional B3LYP[42,43] were carried out using Gaussian 03 program[44]. The 6-31G** basis set[45,46] was used for the main group elements, whereas the Lanl2DZ effective core potential (ECP)[47] was employed for Hg. In vibrational frequency calculations, there was no imaginary frequency for the optimized geometries of **1** and Hg^{2+}-2·**1** complex, suggesting that these geometries represented local minima. For all calculations, the solvent effect of water was considered by using the Cossi and Barone's CPCM (conductor-like polarizable continuum model).[48,49]

3. Results and discussion

*3.1. Synthesis of receptor **1***

Receptor **1** was obtained by the combination of thiosemicarbazide and 8-hydroxyjulolidine-9-carboxaldehyde with 69% yield in ethanol (Scheme 1), and characterized by ^{1}H NMR and ^{13}C NMR, ESI-mass spectrometry, and elemental analysis.

3.2. Fluorescent turn-off detection of Hg^{2+}

Fluorescence monitoring studies of various metal ions by **1** in DMSO/bis-tris buffer (8/2, v/v) at room temperature are shown in Fig. 1. Receptor **1** alone displayed a strong fluorescence emission with an excitation of 385 nm. The addition of some metal ions such as Na^+, K^+, Ag^+, Mg^{2+}, Ca^{2+}, Cr^{3+}, Mn^{2+}, Co^{2+}, Ni^{2+}, Cd^{2+}, Al^{3+}, Ga^{3+} and Pb^{2+} to the solution of **1** showed no significant changes of the fluorescence, while In^{3+}, Fe2+, and Fe^{3+} caused the fluorescence slightly to decrease and Zn^{2+} moved it slightly red-shift. In contrast, the addition of $Hg^{2+}$and Cu^{2+} into **1** resulted in a drastic decrease of the emission intensity at 453 nm. Importantly, **1**-Cu^{2+} complex showed the change of color by naked-eye (Fig. S1). These results indicated that **1**-Hg^{2+} complex could be discriminated from **1**-Cu^{2+} complex by naked-

eye and that **1** could be a suitable chemosensor for both Cu^{2+} and Hg^{2+}.[50]

In order to study in details the fluorescent sensing behavior of **1**, fluorescence titration experiments with Hg^{2+} were performed (Fig. 2). The sensing study of **1** toward Cu^{2+} will be demonstrated elsewhere. When the receptor **1** was titrated with Hg^{2+}, the fluorescence intensity decreased to 1.4 equiv, and no further change was observed. Upon the addition of Hg^{2+} up to 1 equiv, about 90 % of the maximum fluorescence intensity was quenched. The binding properties of **1** with Hg^{2+} were further studied by UV-vis titration experiments (Fig. 3). On the gradual addition of Hg^{2+} to a solution of **1**, the absorption band at 382 nm significantly decreased and a new band at 435 nm increased gradually and reached a maximum at 1 equiv of Hg^{2+}. The isosbestic points were observed at 344 nm and 404, demonstrating that only one product was generated from the interaction of **1** with Hg^{2+}.

The binding mode between **1** and Hg^{2+} was determined through Job plot analysis (Fig. S2).[51] The Job plot exhibited a 1:2 complexation stoichiometry for the Hg^{2+}-2·**1** complex formation. In addition, the formation of the 1:2 complex was confirmed by using ESI-mass spectrometry (Fig. S3). The positive-ion mass spectrum indicated that a peak at m/z = 780.97 was assignable to $[Hg^{2+} + 2\cdot\mathbf{1}(-H^{+}) + \text{solvent}]^{+}$ [calcd. 781.19].

To further get information for the binding mode of **1** with Hg^{2+}, ^{1}H NMR titration study was carried out (Fig. 4). Upon the addition of 1 equiv of Hg^{2+} to **1**, the OH peak of the julolidine moiety at 11.0 ppm and the NH_2 peak of the thiosemicarbazide moiety at 7.8 ppm showed significant downfield shifts, while the rest of the proton signals showed a slight downfield shift. The peaks did not changed upon further addition of Hg^{2+}. These results suggested that the OH of the julolidine moiety or the NH_2 of the thiosemicarbazide moiety might coordinate to Hg^{2+}.

The association constant of Hg^{2+} binding to sensor **1** was found to be 5.0×10^{11} M^{-1} on the basis of Li's equation (Fig. S4).[52] The detection limit of senor **1** as a fluorescent sensor for the detection of Hg^{2+} was determined from a plot of intensity as a function of the concentration of Hg^{2+}. It was found that chemosensor **1** had a detection limit of 0.59 μM on the basis of $3\sigma/K$ (Fig. S5).[53]

To further check the practical applicability of receptor **1** as a Hg^{2+} selective

fluorescence sensor, we carried out competition experiments (Fig. 5). When **1** was treated with 1 equiv of Hg^{2+} in the presence of the same concentration of other metal ions, the fluorescence quenching caused by Hg^{2+} was retained with Na^{+}, K^{+}, Ag^{+}, Mg^{2+}, Cu^{2+}, Ca^{2+}, Cr^{3+}, Mn^{2+}, Fe^{2+}, Fe^{3+}, Co^{2+}, Ni^{2+}, Zn^{2+}, Cd^{2+}, Al^{3+}, Ga^{3+}, In^{3+} and Pb^{2+}. These results indicated that receptor **1** showed an excellent selectivity for mercury in the presence of other metal ions, making it very useful in practical applications.

To understand the sensing mechanisms of **1** toward Hg^{2+}, theoretical calculations were performed with the 1:2 stoichiometry (Hg^{2+} : receptor), based on Job plot and ^{1}H NMR titration. To get the energy-minimized structures of **1** and Hg^{2+}-2·**1** complex, the geometric optimizations of **1** and Hg^{2+}-2·**1** complex were performed by DFT/B3LYP level (S=0, DFT/B3LYP/main group atom: 6-31G** and Hg: Lanl2DZ/ECP). The significant structural properties of the energy-minimized structures were shown in Fig. 6. The energy minimized structure of **1** showed a planar structure with the dihedral angle of 1S, 2C, 3N, 4O = 0.107°, and the hydrogen bond was observed between 3N and 5H (Fig. 6a). Hg^{2+}-2·**1** complex exhibited a slightly tilted structure with the dihedral angle of 1S, 6N, 1'S, 6'N = 44.309°, and Hg^{2+} was coordinated with 1S, 6N, 1'N and 6'N atoms of 2·**1** (Fig. 6b). We further investigated the frontier molecular orbitals of **1** and Hg^{2+}-2·**1** (Fig. S6). In case of **1**, the energy gap between HOMO and LUMO was assigned to ICT band which showed the turn-on fluorescence of **1**. On the other hand, the energy gap between HOMO and LUMO for Hg^{2+}-2·**1** complex was assigned to ligand-to-metal charge-transfer (LMCT), which provided a pathway for non-radiative decay of the excited state.[54] Thus, the chelation of Hg^{2+} showed LMCT, which induced the turn-off fluorescent change of **1**. Based on UV-vis titration, Job plot, ^{1}H NMR titration and theoretical calculations, we proposed the structure of Hg^{2+}-2·**1** complex as shown in Scheme 2.

*3.3. Fluorescent turn-on response of Hg^{2+}-2·**1** complex toward Cys or GSH*

Based on the thiophilic nature of Hg^{2+}, we examined the selectivity of Hg^{2+}-2·**1** complex toward amino acids and peptide. The fluorescent spectral study of Hg^{2+}-2·**1** complex with 20 different amino acids and peptide such as Ala, Asn, Cys, Gln, Glu, Gly, His, Ile, Leu, Lys, Met, Phe, Pro, Ser, Trp, Val, Arg, Thr, Asp and GSH was carried out in DMSO/bis-tris buffer (8/2, v/v) (Fig. 7). The addition of Cys and GSH into the solution of Hg^{2+}-2·**1**

enhanced significantly the intensity of fluorescence emission, while other amino acids showed no change in the emission spectra relative to the free receptor **1**. The fluorescence recovery might be due to release of **1** from the Hg^{2+}-2·**1** complex through the interaction of thiol-containing Cys or GSH with Hg^{2+}. These results showed that Hg^{2+}-2·**1** complex was successfully utilized to probe thiol-containing amino acids with turn-on fluorescence.

To investigate the sensing properties of Cys by Hg^{2+}-2·**1** complex, fluorescence titration was conducted (Fig. 8). On the treatment with Cys to the solution of Hg^{2+}-2·**1**, the fluorescence intensity enhanced gradually and was saturated when the concentration of Cys reached 2 equiv. The absorbance change of Hg^{2+}-2·**1** with Cys was studied by UV-vis titration experiments (Fig. 9). Upon the addition of Cys into the solution of Hg^{2+}-2·**1**, the absorption band at 382 nm steadily increased, and a band at 435 nm gradually decreased. The final UV-vis spectrum was nearly identical to that of sensor **1**, indicating release of **1** from the Hg^{2+}-2·**1** complex. Meanwhile, the isosbestic points were observed at 344 and 404 nm, which indicates the formation of a single species from Hg^{2+}-2·**1** complex upon binding to Cys.

The binding mode between Hg^{2+}-2·**1** and Cys was determined through Job plot analysis (Fig. S7).[51] The Job plot exhibited a 1:1 stoichiometric ratio of Hg^{2+}-2·**1** to Cys. The interactions of Hg^{2+}-2·**1** complex with Cys were analyzed by ESI-mass spectrometry analysis. The positive ion mass spectrum showed that the peak of [**1**+H^+] [calcd 291.13] was observed at *m/z* = 291.19 (Fig. S8). Based on Job plot, UV-vis titrations, and ESI-mass spectrometry analysis, we proposed that a Hg^{2+}-2·**1** complex might undergo the demetallation by Cys (Scheme 3). The binding constant between Hg^{2+}-2·**1** and Cys was calculated as 2.9×10^4 M^{-1} on the basis of Benesi-Hildebrand equation (Fig. S9).[55] Based on the result of fluorescence titration, the detection limit for Cys was determined to be 1.17 μM on basis of 3σ/K (Fig. S10).[53]

The practical applicability of Hg^{2+}-2·**1** complex as a Cys-selective receptor was further ascertained by the competition experiment (Fig. 10). When **1** was treated with 2 equiv of Cys in the presence of the same concentration of other amino acids and peptide, the emission enhancement caused by Cys was retained with Gly, Ala, Ser, Thr, Val, Leu, Ile, Met, Pro, Phe, Trp, Asp, Glu, Asn, Gln, His, Lys, Arg and GSH. There was no interference for the detection of Cys by Hg^{2+}-2·**1** in DMSO/bis-tris buffer (8/2, v/v).

Next, fluorescence titration of Hg^{2+}-2·**1** with GSH was performed to understand the binding property of Hg^{2+}-2·**1** and GSH (Fig. S11). The results were similar to those of Cys. On the treatment with GSH to the solution of Hg^{2+}-2·**1**, the fluorescence intensity enhanced gradually and was saturated when the concentration of GSH reached 2 equiv. The absorbance change of Hg^{2+}-2·**1** with GSH was also studied by UV-vis titration experiments (Fig. S12). Upon the addition of GSH into the solution of Hg^{2+}-2·**1**, the absorption band at 382 nm steadily increased, and a band at 435 nm gradually decreased. The final UV-vis spectrum was also nearly identical to that of sensor **1**, indicating release of **1** from the Hg^{2+}-2·**1** complex. Meanwhile, the isosbestic points were observed at 344 and 404 nm, which indicates the formation of a single species from Hg^{2+}-2·**1** complex upon binding to GSH.

The binding mode between Hg^{2+}-2·**1** and GSH was determined through Job plot analysis (Fig. S13),[51] which exhibited a 1:1 stoichiometric ratio of Hg^{2+}-2·**1** to GSH. Based on UV-vis titrations and Job plot, we proposed that a Hg^{2+}-2·**1** complex might undergo the demetallation by GSH (Scheme 3). The binding constant between Hg^{2+}-2·**1** and GSH was calculated as 6.9×10^3 M^{-1} on the basis of Benesi-Hildebrand equation (Fig. S14).[55] Based on the result of fluorescence titration, the detection limit for GSH was determined to be 1.17 μM on basis of 3σ/K (Fig. S15).[53] Importantly, the detection limit is lowest among those previously reported with Hg^{2+} complexes, to the best of our knowledge.[56-58]

The practical applicability of Hg^{2+}-2·**1** complex as a GSH-selective receptor was further ascertained by the competition experiment (Fig. S16). When Hg^{2+}-2·**1** was treated with 2 equiv of GSH in the presence of the same concentration of other amino acids and peptide, the emission enhancement caused by GSH was retained with Gly, Ala, Ser, Thr, Val, Leu, Ile, Met, Pro, Phe, Trp, Asp, Glu, Asn, Gln, His, Lys, Arg and Cys. There was no interference for the detection of GSH by Hg^{2+}-2·**1** in DMSO/bis-tris buffer (8/2, v/v).

On the other hand, it would be very useful to discriminate Cys from GSH by **1**-Hg^{2+} complex. As shown in Fig. S17, **1**-Cu^{2+} complex with a yellow color underwent demetallation by only Cys to give a colorless Cu-Cys complex, while it did not react with GSH, resulting in no color change. If the solution color of **1**-Hg^{2+} complex containing Cys or GSH in the presence of Cu^{2+} would change from yellow to colorless, then, we could tell that the solution contains Cys. In contrast, if the solution color of **1**-Hg^{2+} complex would show no change,

then, GSH might exist in the solution.

Conclusion.

We have developed a new sensor **1** for the sequential detection of Hg^{2+} and Cys or GSH. Receptor **1** exhibited obviously Hg^{2+}-selective ON-OFF fluorescence quenching behavior together with a decrease of the emission intensity by Cu^{2+} and a red-shift of it by Zn^{2+}. The fluorescence quenching with Hg^{2+} was explained by theoretical calculations. Chemosensor **1** is advantageous in terms of its sufficiently low detection limit (0.59 μM) for detection of trace amounts of Hg^{2+} ion present in many chemical and biological systems and its high selectivity in the presence of potential competitors such as Ag^{+} and Pb^{2+}. Moreover, the resulting Hg^{2+}-2·**1** complex was used as OFF-ON fluorescent sensor for Cys or GSH by using the property of the mercury-sulfur affinity. In particular, the detection limit for GSH (1.17 μM) is lowest among those previously reported with Hg^{2+} complexes, to the best of our knowledge. We believe that this Schiff base sensor could be a guidance to the development of a new type of the sequential recognition of Hg^{2+} and thiol-containing amino acids.

Acknowledgements

Financial support from Basic Science Research Program through the National Research Foundation of Korea (NRF) funded by the Ministry of Education, Science and Technology (NRF-2014R1A2A1A11051794 and NRF-2015R1A2A2A09001301) are gratefully acknowledged.

Appendix A. Supplementary data

Supplementary data related to this article can be found at http://????.

References

1. A. P. de Silva , H. Q. N. Gunaratne, T. Gunnlaugsson , A. J. M. Huxley, C. P. McCoy , J. T. Rademacher and T. E. Rice, *Chem. Rev.*, 1997, **97**, 1515-1566.
2. J.-P. Desvergne and A. W. Czarnik, in Chemosensors of Ion and Molecular Recognition, Kluwer, Dordrecht, 1997
3. B. Valeur and I. Leray, *Coord. Chem. Rev.*, 2000, **205**, 3-40.
4. L. Prodi, F. Bolletta, M. Montalti and N. Zaccheroni, *Coord. Chem. Rev.*, 2000, **205**, 59-83.
5. H. N. Kim, W. X. Ren, J. S. Kim and J. Yoon, *Chem. Soc. Rev.*, 2012, **41**, 3210-3244.
6. H. H. Harris, I. J. Pickering and G. N. George, *Science*, 2003, **301**, 1203.
7. P. B. Tchounwou, W. K. Ayensu, N. Ninashvili and D. Sutton, *Environ. Toxicol.*, 2003, **18**, 149-175
8. J. H. Kim, J. Y. Noh, I. H. Hwang, J. J. Lee and C. Kim, *Tetrahedron Lett.*, 2013, **54**, 4001-4005
9. Y. W. Choi, G. R. You, M. M. Lee, J. Kim, K.-D. Jung and C. Kim, *Inorg. Chem. Commun.*, 2014, **46,** 43-46.
10. J. K. Virtanen, T. H. Rissanen, S. Voutilainen and T. P. Tuomainen, *J. Nutr. Biochem.*, 2007, **18**, 75-85.
11. T. W. Clarkson, L. Magos and G. J. Myers, *New Engl. J. Med.*, 2003, **349**,1731-1737.
12. E. Shigeo, S. Mari, N. Tadashi, I. Keiko and K. Toshinori, *J. Neurol. Sci.*, 2007, **262**, 131-144.
13. Y. Takashi, K. Saori, T. Toshihide and H. Masazumi, *Sci. Total Environ.*, 2009, **408**, 272-

276.

14. Y. W. Chen, C. F. Huang, K. S. Tsai, R. S. Yang, C. C. Yen, C. Y. Yang, S. Y. Lin-Shiau and S. H. Liu, *Chem. Res. Toxicol.*, 2006, **19**, 1080-1085.

15. P. Holmes, K. A. F. James and L. S. Levy, *Sci. Total Environ.*, 2009, **408**, 171-182.

16. R. O. Ball, G. Courtney-Martin and P. B. Pencharz, *J. Nutr.*, 2006, **136**, 1682S-1693S.

17. O. W. Griffith, *Methods Enzymol.*, 1987, **143**, 366-368.

18. Y. W. Choi, J. J. Lee, G. R. You and C. Kim, *RSC Adv.*, 2015, **5**, 38308-38315.

19. S. A. Lee, J. J. Lee, J. W. Shin, K. S. Min and C. Kim, *Dyes Pigments*., 2015, **116**, 131-138.

20. Y. S. Kim, G. J. Park. S. A. Lee and C. Kim, *RSC Adv*., 2015, **5**, 31179-31188.

21. R. Janaky, V. Varga, A. Hermann, P. Saransaari and S.S. Oja, *Neurochem. Res.,* 2000, **25**, 1397-1405.

22. X. F. Wang and M. S. Cynader, *J. Neurosci.*, 2001, **21**, 3322-3331.

23. N. Saravanan, D. Senthil and P. Varalakshmi, *Br. J. Urol.*, 1996, **78**, 22-24.

24. S. Shahrokhian, *Anal. Chem.*, 2001, **73**, 5972-5978.

25. S. C. Lu, Mol. *Aspects Med.*, 2009, **30**, 42-59.

26. D. M. Townsend, K. D. Tew and H. Tapiero, *Biomed. Pharmacother.*, 2003, **57**, 145-155.

27. C. L. Gatlin and F. Turecek, *J. Mass Spectrom*., 2000, 35, 172–7.

28. L. Xu, Y. Xu, W. Zhu, B. Zeng, C. Yang, B. Wu and X. Qian, *Org. Biomol. Chem*., 2011, 9, 8284–7.

29. R. K. Pathak, J. Dessingou and C. P. Rao, *Anal. Chem*., 2012, 84, 8294–300.

30. J. Zhao, C. Chen, L. Zhang, J. Jiang, G. Shen and R. Yu, *Analyst*, 2013, 138, 1713–8.

31. J. Du, J. Fan, X. Peng, P. Sun, J. Wang, H. Li and S. Sun, *Org. Lett*., 2010, 12, 476–9.

32. J. Du, J. Fan, X. Peng, P. Sun, J. Wang, H. Li and S. Sun, *Org. Lett*., 2010, 12, 476–9.

33. Y.-B. Ruan, A.-F. Li, J.-S. Zhao, J.-S. Shen and Y.-B. Jiang, *Chem. Commun*., 2010, 46, 4938–40.

34. J. Wu, R. Sheng, W. Liu, P. Wang, J. Ma, H. Zhang and X. Zhuang, *Inorg. Chem*., 2011, 50, 6543–51.

35. L. Ma, G. Wu, Y. Li, P. Qin, L. Meng, H. Liu, Y. Li and A. Diao, *Nanoscale*, 2015, 7, 18044–8.

36. J. Zhang, J. Tian, Y. He, Y. Zhao and S. Zhao, *Chem. Commun*., 2014, 50, 2049–51.

37. E. Chekmeneva, J. M. Díaz-Cruz, C. Ariño and M. Esteban, *J. Electroanal. Chem*., 2010, 644, 20–24.

38. Y. Xu, X. Niu, H. Zhang, L. Xu, S. Zhao, H. Chen and X. Chen, *J. Agric. Food Chem*., 2015, 63, 1747–55.

39. H. Xu, S. Huang, C. Liao, Y. Li, B. Zheng, J. Du and D. Xiao, *RSC Adv.*, 2015, 5, 89121–89127.

40. X. Chen, S.-W. Nam, M. J. Jou, Y. Kim, S.-J. Kim, S. Park and J. Yoon, *Org. Lett.*, 2008, **10**, 5235-5238.

41. F. J. Huo, Y. Q. Sun, J. Su, J. B. Chao, H. J. Zhi and C. X. Yin, *Org. Lett.*, 2009, **11**, 4918-4921.

42. A. D. Becke, *J. Chem. Phys.*, 1993, **98**, 5648-5652.

43. C. Lee, W. Yang and R.G. Parr, *Phys. Rev. B*, 1988, **37**, 785-789.

44. M.J. Frisch, G.W. Trucks, H.B. Schlegel, G.E. Scuseria, M.A. Robb, J.R. Cheeseman, J.A. Montgomery, Jr., T. Vreven, K.N. Kudin, J.C. Burant, J.M. Millam, S.S. Iyengar, J. Tomasi, V. Barone, B. Mennucci, M. Cossi, G. Scalmani, N. Rega, G.A. Petersson, H. Nakatsuji, M. Hada, M. Ehara, K. Toyota, R. Fukuda, J. Hasegawa, M. Ishida, T.

Nakajima, Y. Honda, O. Kitao, H. Nakai, M. Klene, X. Li, J.E. Knox, H.P. Hratchian, J.B. Cross, V. Bakken, C. Adamo, J. Jaramillo, R. Gomperts, R.E. Stratmann, O. Yazyev, A.J. Austin, R. Cammi, C. Pomelli, J.W. Ochterski, P.Y. Ayala, K. Morokuma, G.A. Voth, P. Salvador, J.J. Dannenberg, V.G. Zakrzewski, S. Dapprich, A.D. Daniels, M.C. Strain, O. Farkas, D.K. Malick, A.D. Rabuck, K. Raghavachari, J.B. Foresman, J.V. Ortiz, Q. Cui, A.G. Baboul, S. Clifford, J. Cioslowski, B.B. Stefanov, G. Liu, A. Liashenko, P. Piskorz, I. Komaromi, R.L. Martin, D.J. Fox, T. Keith, M.A. Al-Laham, C.Y. Peng, A. Nanayakkara, M. Challacombe, P.M.W. Gill, B. Johnson, W. Chen, M.W. Wong, C. Gonzalez, and J.A. Pople, Gaussian 03, Revision D.01, Gaussian, Inc., Wallingford CT, 2004.

45. P. J. Hay and W. R. Wadt, *J. Chem. Phys.*, 1985, **82**, 270-283.

46. P. J. Hay and W. R. Wadt, *J. Chem. Phys.*, 1985, **82**, 284-298.

47. P. J. Hay and W. R. Wadt, *J. Chem. Phys.*, 1985, **82**, 299-310.

48. V. Barone and M. Cossi, *J. Phys. Chem. A*, 1998, **102**, 1995-2001.

49. M. Cossi and V. Barone, *J. Chem. Phys.*, 2001, **115**, 4708-4717.

50. One of the referees raised a question on how to determine the concentration of Hg^{2+} in the presence of a small amount of Cu^{2+} in a sample. Fortunately, **1**-Hg^{2+} complex undergoes demetallation with I^- to regenerate the sensor **1**, resulting in the regeneration of the original fluorescence of **1**, while **1**-Cu^{2+} complex does not react with I^- (Fig. S18). In case of the mixture solution containing both **1**-Cu^{2+} and **1**-Hg^{2+} complexes, therefore, I^- would be added into the solution. Then, **1** would be released from only **1**-Hg^{2+} complex, and showed the recovery of the fluorescence. The concentration of Hg^{2+} in the presence of a small amount of Cu^{2+} could be determined from the fluorescence recovery.

51. P. Job, *Ann. Chim.*, 1928, **9,** 113-203.

52. G. Grynkiewicz, M. Poenie and R. Y. Tsien, *J. Biol. Chem.*, 1985, **260**, 3440-3450.

53. Y.-K. Tsui, S. Devaraj and Y.-P. Yen, *Sens. Actuators B*, 2012, **161**, 510-519.

54. H. S. Jung, P. S. Kwon, J. W. Lee, J. I. Kim, C. S. Hong, J. W. Kim, S. Yan, J. Y. Lee, J. H. Lee, T. Joo and J. S. Kim, *J. Am. Chem. Soc.*, 2009, **131**, 2008-2012.

55. H. A. Benesi and J. H. Hildebrand, *J. Am. Chem. Soc.*, 1949, **71**, 2703-2707.

56. Y. Zeng, G. Zhang, D. Zhang and D. Zhu, *Tetrahedron Lett.*, 2008, **49**, 7391-7394.

57. R. Peng, L. Lin, X. Wu, X. Liu and X. Feng, *J. Org. Chem.*, 2013, **78**, 11602-11605.

58. K. Ghosh, D. Tarafdar, A. Samadder and A. R. Khuda-Bukhsh, *New J. Chem.*, 2013, **37**, 4206-4213.

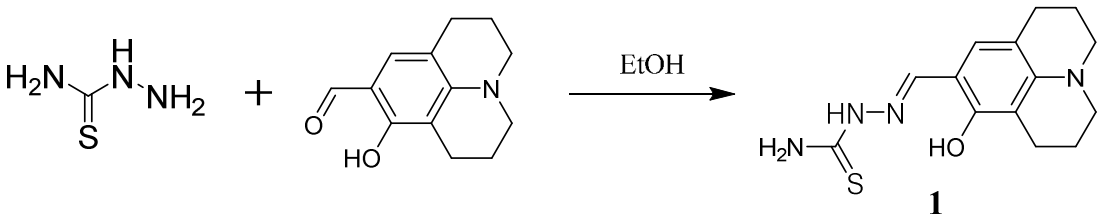

Scheme 1. Synthetic procedure of **1**.

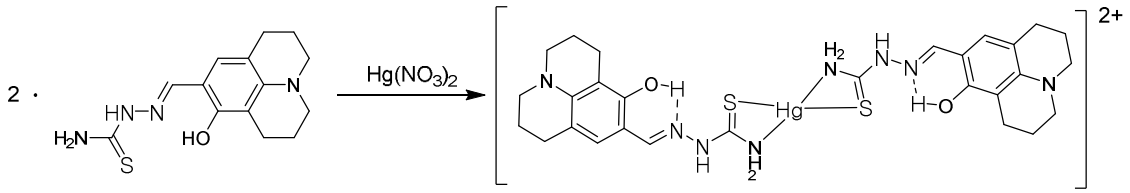

Scheme 2. Proposed binding mode of Hg^{2+}-2·**1** complex.

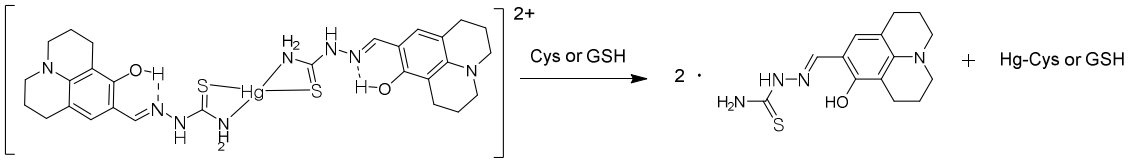

Scheme 3. Proposed sensing mechanism of Cys or GSH by Hg^{2+}-2·**1** complex.

Figure captions

Fig. 1 Fluorescence spectra of **1** (10 μM) upon the addition of 1 equiv of various metal ions in DMSO/bis-tris buffer (8/2, v/v).

Fig. 2 Fluorescence spectral changes of **1** (10 μM) in the presence of different concentrations of Hg^{2+} ions in DMSO/bis-tris buffer (8/2, v/v). Inset: Fluorescence intensity at 453 nm versus the number of equiv of Hg^{2+} added.

Fig. 3 Absorption spectral changes of **1** (10 μM) after addition of increasing amounts of Hg^{2+} in DMSO/bis-tris buffer (8/2, v/v). Inset: Absorption at 382 nm versus the number of equiv of Hg^{2+} added.

Fig. 4 ^1H NMR titration of **1** with Hg^{2+}.

Fig. 5 Competitive selectivity of **1** (10 μM) toward Hg^{2+} (1 equiv) in the presence of other metal ions (1 equiv) in DMSO/bis-tris buffer (8/2, v/v).

Fig. 6 The energy-minimized structures of (a) **1** and (b) Hg^{2+}-2·**1** complex.

Fig. 7 Fluorescence spectral changes of Hg^{2+}-2·**1** upon addition of 2 equiv of various amino acids and peptide.

Fig. 8 Fluorescence spectral changes of Hg^{2+}-2·**1** in the presence of different concentrations of Cys in DMSO/bis-tris buffer (8/2, v/v). Inset: Fluorescence intensity at 453 nm versus the number of equiv of Cys added.

Fig. 9 Absorption spectral changes of Hg^{2+}-2·**1** after addition of increasing amounts of Cys in DMSO/bis-tris buffer (8/2, v/v). Inset: Absorption at 382 nm versus the number of equiv of Cys added.

Fig. 10 Competitive selectivity of Hg^{2+}-2·**1** toward Cys (2 equiv) in the presence of other amino acids and peptide (2 equiv) in DMSO/bis-tris buffer (8/2, v/v)

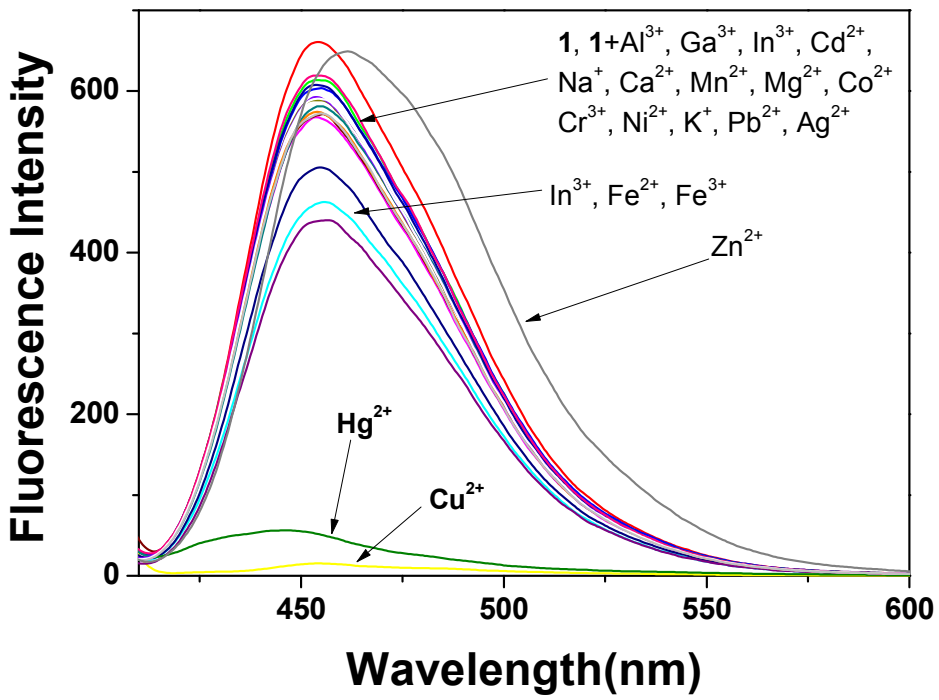

Fig. 1

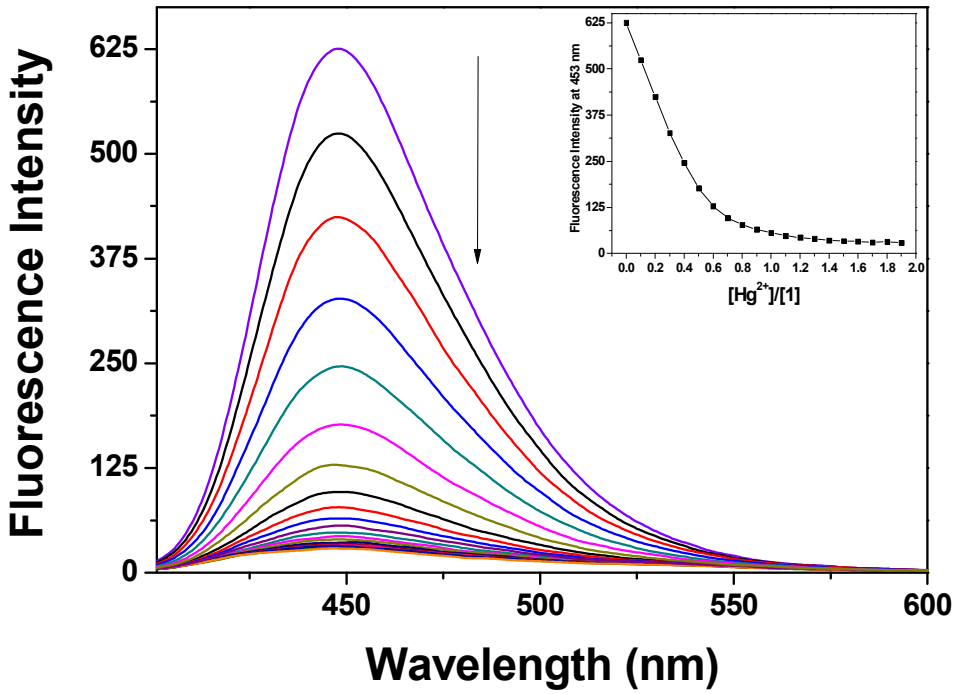

Fig. 2

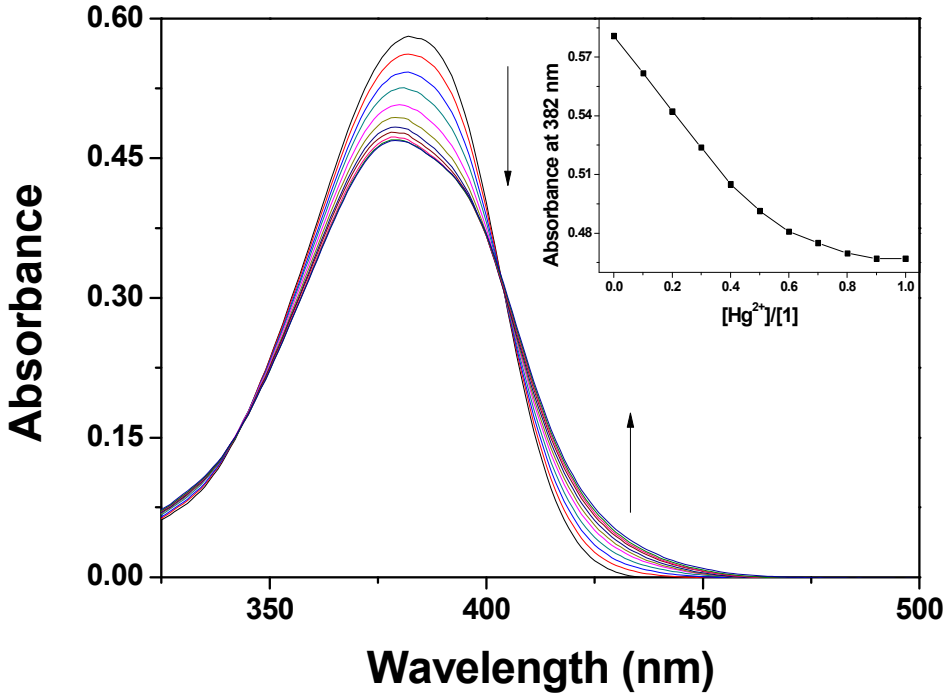

Fig. 3

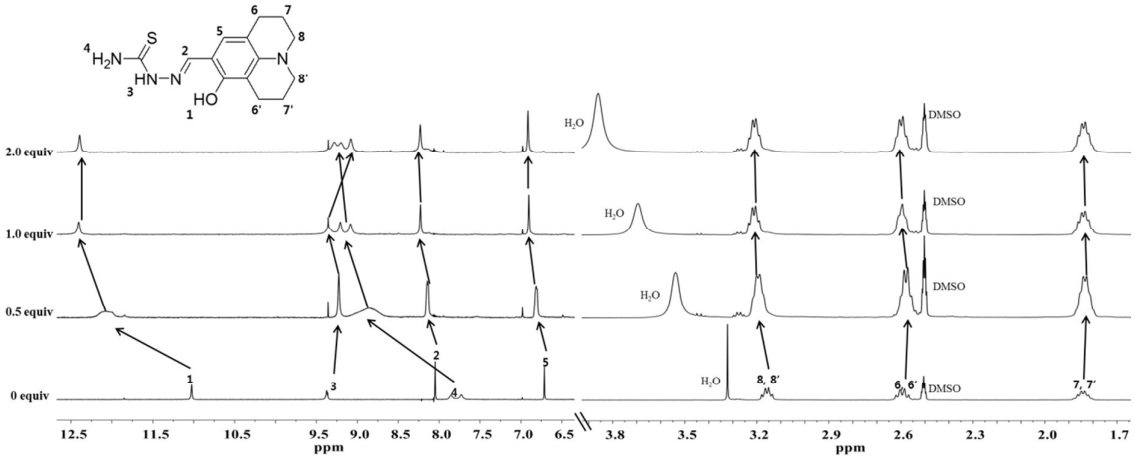

Fig. 4

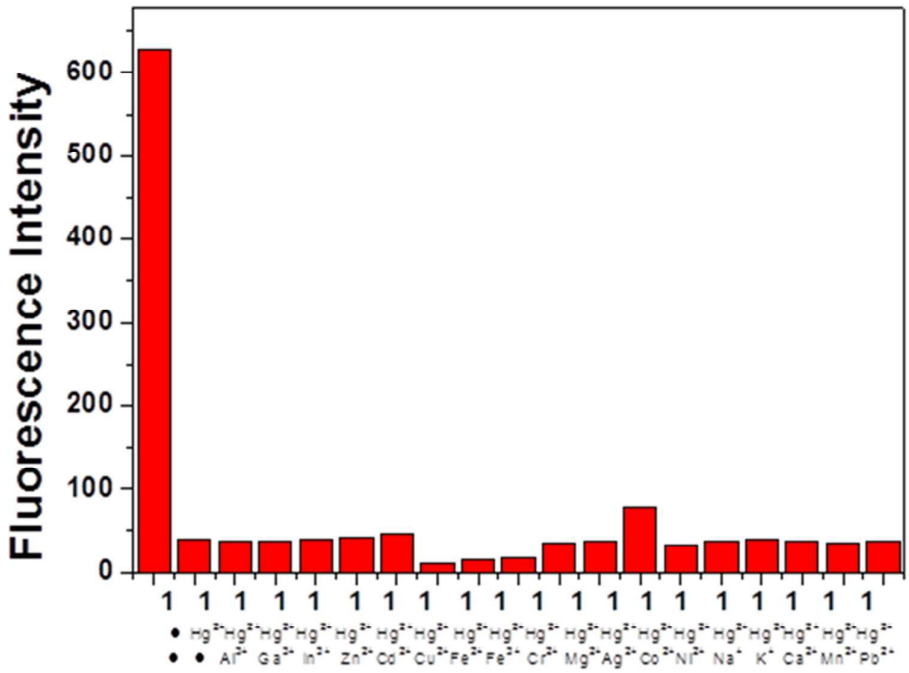

Fig. 5

(a)

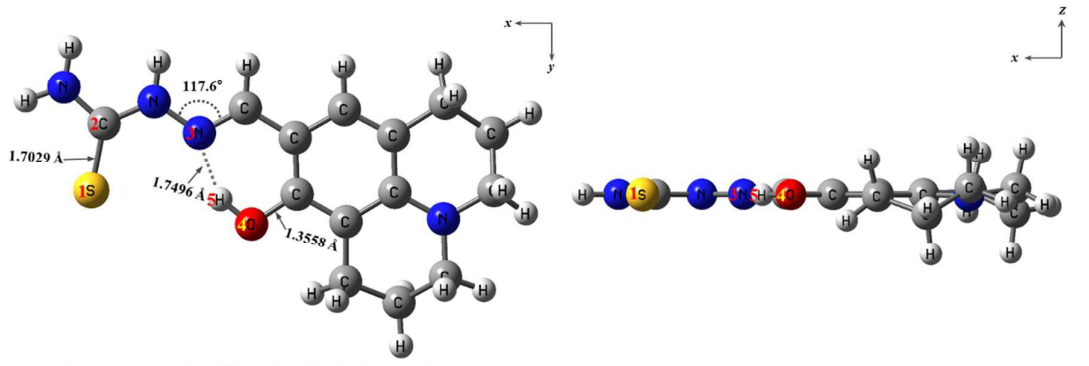

Dihedral angle (1S, 2C, 3N, 4O) : 0.107°

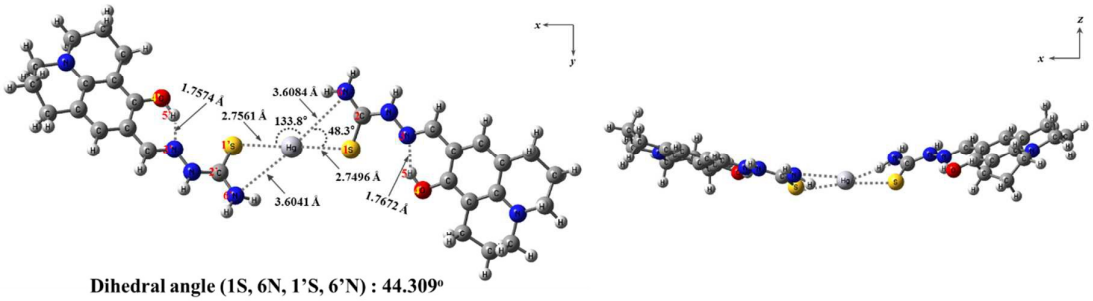

Dihedral angle (1S, 6N, 1'S, 6'N) : 44.309°

(b)

Fig. 6

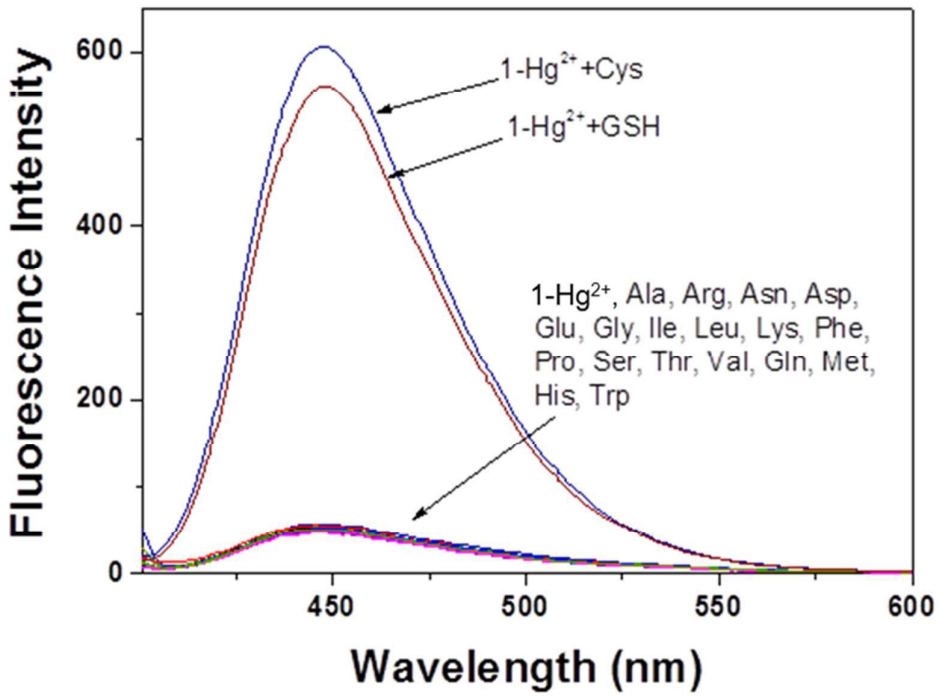

Fig. 7

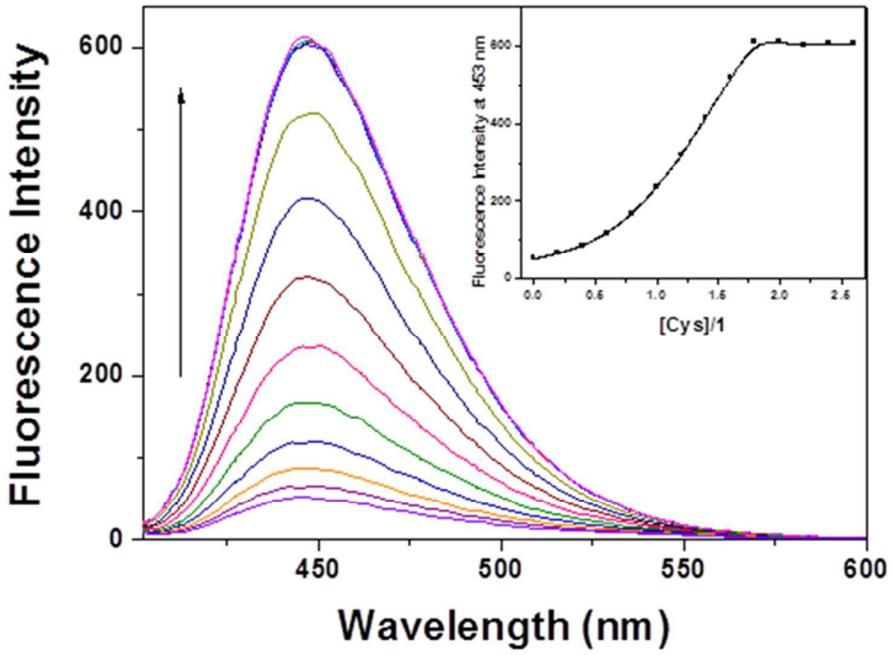

Fig. 8

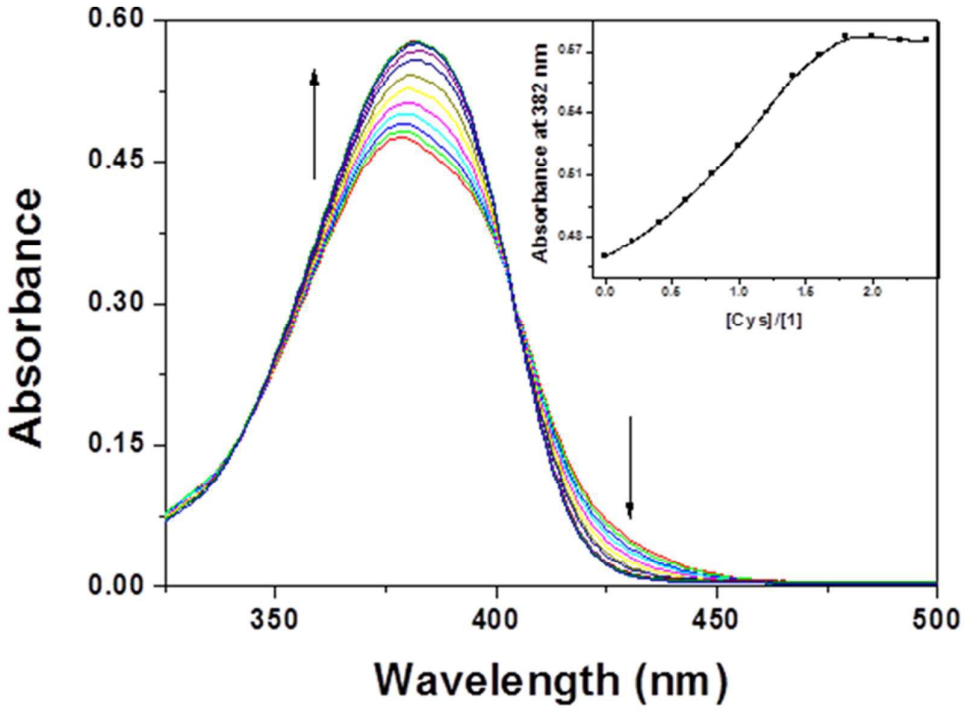

Fig. 9

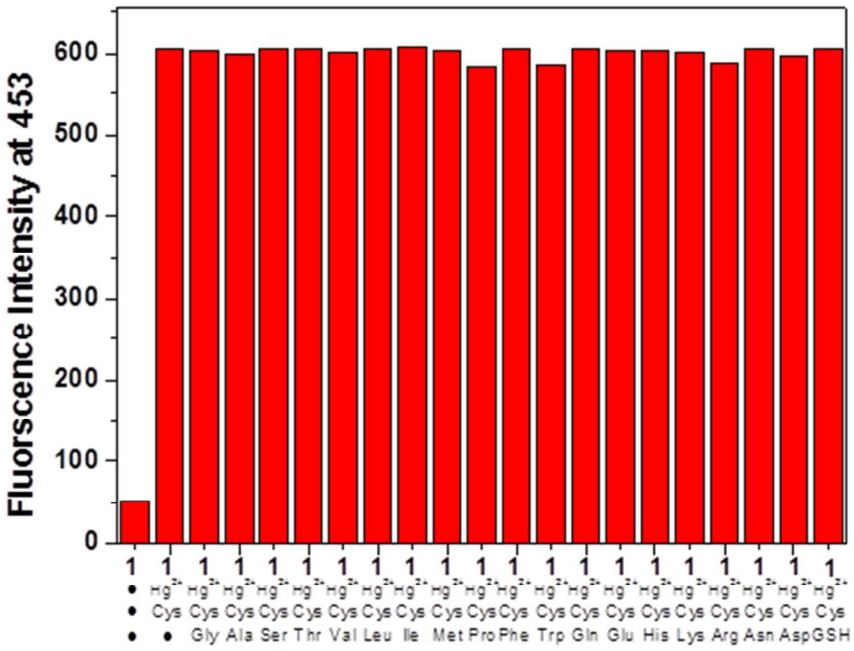

Fig. 10

Graphical abstract

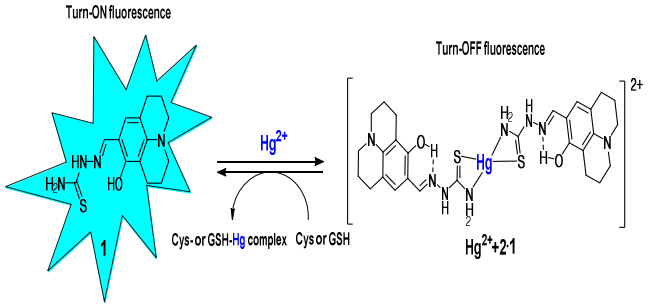

A selective fluorescent chemosensor **1** was developed for the sequential detection of Hg^{2+} and cysteine or glutathione.